

Boundary-induced energy localization in a nonlinear quantum lattice

Vincent Pouthier*

Institut UTINAM, UMR CNRS 6213, Université de Franche-Comté, 25030 Besançon cedex, France
(Received 19 July 2007; revised manuscript received 2 November 2007; published 19 December 2007)

The dynamics of v bosons initially created on the same site of a finite-size lattice is analyzed according to a Bose version of the Hubbard model. For a boson number greater than 2, it is shown that the interplay between symmetry breaking and nonlinearity favors the occurrence of localized bound states. In a localized state, the v bosons are trapped close to each other and they behave as a single particle whose wave function is exponentially localized near a lattice side. Consequently, the creation of v bosons on a side site mainly excites a localized state so that the main part of the energy stays localized on the excited site over an infinite time scale.

DOI: [10.1103/PhysRevB.76.224302](https://doi.org/10.1103/PhysRevB.76.224302)

PACS number(s): 63.20.Ry, 63.20.Pw, 03.65.Ge

I. INTRODUCTION

The concept of energy localization due to nonlinearity in classical lattices has been a central topic of intense research over the last three decades. In that context, the discrete version of the nonlinear Schrödinger (DNLS) equation plays a key role due to its relevance to interpret a large number of phenomena. For instance, the DNLS equation has been used to describe the vibrational energy flow in α -helices,¹⁻³ the dynamics of local modes in small molecules,⁴ the coupling between optical wave guides,⁵ and the trapping of a Bose-Einstein condensate in optical lattices.^{6,7} This equation has revealed the occurrence of a remarkable feature known as the self-trapping mechanism,^{8,9} which is a special example of a more general solution called discrete breathers.¹⁰⁻¹³ In classical lattices with translational invariance, discrete breathers are generic time-periodic and spatially localized solutions which result from the interplay between the discreteness and the nonlinearity. Since they sustain a local accumulation of the energy, which might be pinned in the lattice or may travel through it, they are expected to be of fundamental importance.

At present, because the occurrence of classical breathers is a relatively well-understood phenomenon, a great attention has been paid to characterize their quantum equivalent.¹⁴ Most of the theoretical analysis was performed within the quantum equivalent of the DNLS equation. The corresponding Hamiltonian is essentially a Bose version of the Hubbard model which has been used to study a great variety of situations including molecular lattice dynamics,^{15,16} vibrations in adsorbed monolayer,¹⁷ energy flow in α -helices,¹⁸⁻²⁰ and Bose-Einstein condensates.²¹⁻²³ Within this model, nonlinearity is responsible for a strong interaction between bosons located on the same site. It leads to the occurrence of specific states called multiquantum bound states^{14-20,24-31} which have been observed in various molecular adsorbates³²⁻⁴⁰ and in α -helices.^{41,42}

A bound state corresponds to the trapping of several quanta over only a few neighboring sites, with a resulting energy which is less than the energy of quanta lying far apart. The distance separating the quanta is small, so that they behave as a single particle delocalized along the lattice with a well-defined momentum. Although bound states cannot localize the energy because they must share the symme-

try of the translation operator, they take a very long time to tunnel from one lattice site to another. In other words, the initial excitation of several quanta on a single site produces a localization of the energy over a time scale that increases with both the nonlinearity and the number of bosons. This localized behavior, known as the quantum signature of classical self-trapping, disappears in the long-time limit due to the nonvanishing dispersion of the bound-state energy band.

In the present paper, a new facet of bound states is explored through the study of a finite-size nonlinear quantum lattice with open boundaries. Indeed, it is well known that the confinement of a single boson prevents the occurrence of Bloch waves due to the multiple reflections induced by the lattice sides. The true eigenstates are superimpositions of incident and reflected plane waves so that a stationary regime takes place as in a resonant cavity. By contrast, when several quanta are excited, translational symmetry breaking is responsible for a surprising effect since multiboson bound states may localize on each lattice side. This effect originates in the interplay between nonlinearity and the presence of a lattice side. It favors the accumulation of energy over an infinite time scale, leading to the occurrence of a true quantum self-trapping. However, as will be shown in this paper, the bound states localize when the number of bosons is greater than a critical value equal to 2. At this step let us mention that the energy localization at the edge of a classical nonlinear lattice has been demonstrated both theoretically and experimentally in a self-focusing optical device. Such discrete surface modes can be viewed as discrete solitons trapped at the edge of a waveguide array when the beam power exceeds a certain critical value associated with a strong repulsive surface energy (see for instance Refs. 43-49).

The paper is organized as follows. In Sec. II, the general properties of the Hubbard model are summarized and the quantum dynamics required to characterize the energy transfer is introduced. The corresponding time-dependent Schrödinger equation is solved numerically in Sec. III where a detailed analysis of the dynamics is performed. Finally, the numerical results are discussed and interpreted in Sec. IV.

II. MODEL HAMILTONIAN AND QUANTUM ANALYSIS

A. Hamiltonian and quantum states

We consider a finite-size one-dimensional lattice whose N sites $n=1, \dots, N$ contain high-frequency oscillators described by the standard boson operators b_n^\dagger and b_n . The lattice dynamics is governed by a Hubbard model for bosons whose Hamiltonian is written as (using the convention $\hbar=1$)

$$H = \sum_{n=1}^N \omega_0 b_n^\dagger b_n - A b_n^{\dagger 2} b_n^2 + \sum_{n=1}^{N-1} \Phi [b_n^\dagger b_{n+1} + b_{n+1}^\dagger b_n], \quad (1)$$

where ω_0 is the internal frequency of each oscillator, Φ is the hopping constant between nearest-neighbor sites, and A represents the positive nonlinearity.

Since H [Eq. (1)] conserves the number of quanta, its eigenstates can be determined by using the number state method detailed in Ref. 27. To proceed, the Hilbert space E is partitioned into independent subspaces as $E = E_0 \oplus E_1 \oplus E_2 \oplus \dots \oplus E_v \oplus \dots$, where E_v refers to the v -boson subspace. To generate E_v , a useful basis set is formed by the local vectors $|p_1, \dots, p_N\rangle$ ($\sum_n p_n = v$), where p_n is the number of bosons located on the n th site. The dimension d_v of E_v is equal to the number of ways of distributing v indistinguishable quanta among N sites—i.e., $d_v = (N+v-1)!/v!(N-1)!$. Within this representation H is block diagonal. In each subspace E_v , the corresponding Schrödinger equation can be solved numerically to determine the eigenvalues $\omega_\alpha^{(v)}$ and the associated eigenvectors $|\Psi_\alpha^{(v)}\rangle$ labeled by the index $\alpha = 1, \dots, d_v$.

In a general way, the dimension of E_v increases exponentially with both the lattice size and the boson number. For instance, for $N=30$, the dimension of E_3 is equal to $d_3 = 4960$ whereas the dimension of E_4 reaches $d_4 = 40\,920$. Therefore, to limit the computational effort, we shall restrict our attention to the three situations $v=1, 2$, and 3 . As will be shown in the next sections, this restriction is sufficient to highlight the occurrence of localized bound states.

B. Quantum dynamics

The quantum dynamics is governed by the time-dependent Schrödinger equation written as

$$i \frac{d|\Psi(t)\rangle}{dt} = H|\Psi(t)\rangle, \quad (2)$$

where $|\Psi(t)\rangle$ is the lattice quantum state at time t . To solve Eq. (2), we consider the initial creation of v bosons on the (n_0) th site as

$$|\Psi(0)\rangle = \frac{b_{n_0}^{\dagger v}}{\sqrt{v!}}|0\rangle, \quad (3)$$

where $|0\rangle$ denotes the vacuum with zero quanta.

This specific choice allows us to characterize the ability of the nonlinear quantum lattice to localize the energy. Indeed, when $n_0=N/2$ and for a sufficiently large lattice, the creation of v quanta on a single site excites preferentially the so-called soliton band which describes v bosons trapped on

the same site and which behaves as a single particle.^{26,27} Because the dispersion of this band scales as $v\Phi^v/(v-1)!A^{v-1}$ when $A \gg \Phi$, the v quanta are localized in the vicinity of the excited site over a time scale which increases with both A and v . This quantum signature of the classical self-trapping disappears in the long-time limit due to the finite dispersion of the soliton band. By contrast, when $n_0=1$, the v bosons are created on a lattice side. Such an initial condition explicitly accounts for the translational symmetry breaking and it allows us to analyze the way the quantum self-trapping is modified by the confinement.

To characterize the dynamics, several observables are introduced. First, information about the way the energy is distributed along the lattice is given by the expectation value of the population operator defined as

$$g_n(t) = \langle \Psi(t) | b_n^\dagger b_n | \Psi(t) \rangle. \quad (4)$$

Then, the survival probability $P_{n_0}(t) = |\langle \Psi(0) | \Psi(t) \rangle|^2$, which defines the probability to observe the lattice in the state $|\Psi(0)\rangle$ at time t , characterizes the lattice memory of the initial localized state. It is expressed in terms of the Fourier transform of the local density of state (LDOS) $\rho_{n_0}(\omega)$ as

$$P_{n_0}(t) = \left| \int_{-\infty}^{+\infty} \rho_{n_0}(\omega) e^{-i\omega t} d\omega \right|^2, \quad (5)$$

where $\rho_{n_0}(\omega)$ describes the weight of the initial state in the lattice eigenstates whose energy ranges between ω and $\omega + d\omega$ as

$$\rho_{n_0}(\omega) = \sum_{\alpha} |\langle \Psi_\alpha^{(v)} | \Psi(0) \rangle|^2 \delta(\omega - \omega_\alpha^{(v)}). \quad (6)$$

In the next section, this formalism is applied to study the time evolution of the finite-size quantum lattice. The numerical diagonalization of the Hamiltonian H is performed and the time-dependent Schrödinger equation is solved. From knowledge of the corresponding eigenvalues and eigenvectors, the different observables are computed by using Eqs. (4)–(6).

III. NUMERICAL RESULTS

To realize the simulation, the hopping constant Φ is used as a reduced unit and the nonlinearity A is taken as a free positive parameter.

In Fig. 1, the time evolution of the survival probability is displayed for $v=1$ and $N=100$ and for $n_0=N/2$ (black line) and $n_0=1$ (gray line). Whatever the position of the excited site, $P_{n_0}(t)$ decays according to time which indicates that the boson is not localized. When $n_0=N/2$, the survival probability shows damped oscillations and its first zero is reached for $t \approx 1.2\Phi^{-1}$. The time scale reported in the figure is not large enough to observe the reflections so that the boson behaves as in an infinite lattice. It delocalizes along the lattice according to a superimposition of plane waves whose average group velocity is typically of about Φ . When $n_0=1$, a slower decay takes place in the short-time limit. Nevertheless, $P_{n_0}(t)$ does not exhibit significant oscillations. It rapidly vanishes and it is almost equal to zero once $t > 4\Phi^{-1}$.

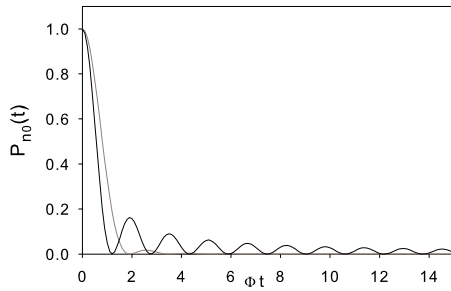


FIG. 1. (Color online) Time evolution of the survival probability for $v=1$, $N=100$, $n_0=N/2$ (black line), and $n_0=1$ (gray line).

The space and time evolution of the boson population is shown in Fig. 2 for $v=2$, $A=3.0$, and $N=61$. When $n_0=N/2$ [Fig. 2(a)], the population of the excited site decreases slowly. It exhibits damped oscillations and its first zero is reached for $t \approx 4\Phi^{-1}$. This decay is accompanied by the emission of two wave packets on each side of the central site. These wave packets propagate rather slowly and they reach the lattice sides at time $t \approx 50\Phi^{-1}$. Similar features are observed when a side site is excited [Fig. 2(b)]. However, because of the symmetry breaking, only one wave packet is emitted from the lattice side. It propagates rather slowly and it reaches the other side of the lattice at time $t \approx 100\Phi^{-1}$.

The corresponding survival probability is shown in Fig. 3 for $A=1.0$ (dashed black line), $A=3.0$ (solid black line), and

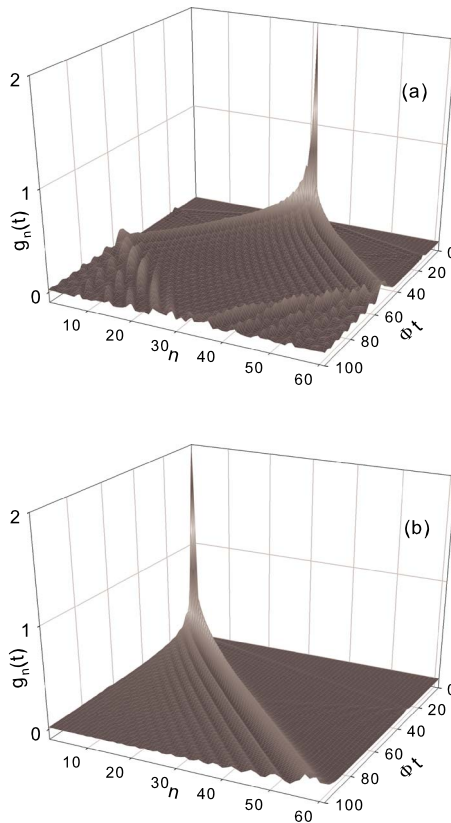


FIG. 2. (Color online) Space and time evolution of the boson population for $v=2$, $A=3.0$, and $N=61$ and for (a) $n_0=N/2$ and (b) $n_0=1$.

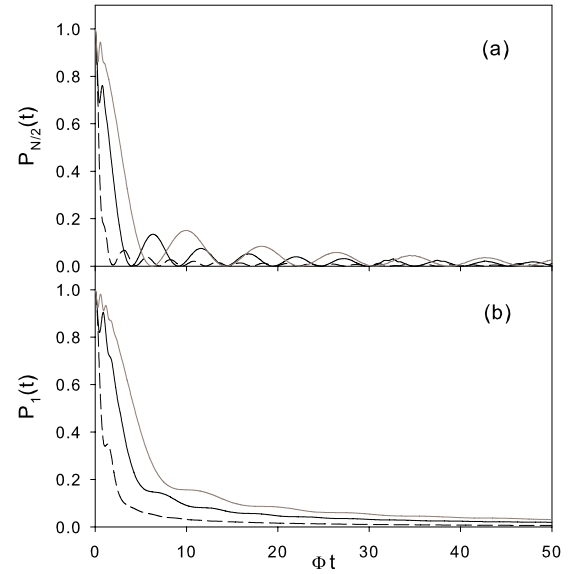


FIG. 3. (Color online) Time evolution of the survival probability for $v=2$ and for $A=1.0$ (dashed black line), $A=3.0$ (solid black line), and $A=5.0$ (solid gray line). (a) $n_0=N/2$ and (b) $n_0=1$.

$A=5.0$ (solid gray line). When $n_0=N/2$ [Fig. 3(a)], $P_{n_0}(t)$ shows damped oscillations whose both damping rate and frequency decrease with A . For $A=1, 3$, and 5 , the first zero is reached for $t=1.8\Phi^{-1}$, $4.0\Phi^{-1}$, and $6.2\Phi^{-1}$, respectively. As shown in Fig. 3(b), the survival probability of the side site behaves similarly to that of the central site. It basically decays over the same time scale but it does not exhibit any oscillation.

Figure 4(a) displays the LDOS versus the eigenenergies for $v=2$, $A=3.0$, $N=61$, and $n_0=1$. Note that the eigenenergies are centered on $\epsilon_0=2\omega_0-2A$. The energy spectrum supports two bands. The numerical analysis of the corresponding eigenvectors reveals that the low-frequency band refers to two-boson bound states. By contrast, the high-frequency band characterizes free states involving two independent bosons. Therefore, as in a lattice with translational invariance, the initial localization of two bosons on a side site preferentially excites the bound-state band. Nevertheless, this excitation is not symmetric since the LDOS is maximum in the high-frequency edge of the band. Consequently, the energy is transported by two-boson bound states whatever the position of the excited site. According to the standard quantum self-trapping theory, these bound states delocalize along the lattice with an average group velocity of about Φ^2/A , which corroborates the results observed in the previous figures. Note that the inset of Fig. 4(a) reveals that free states are also excited, but to a lesser extent.

As shown in Fig. 5 for $A=3.0$ and $N=31$, a fully different behavior takes place when the boson number is equal to $v=3$. Indeed, when $n_0=N/2$ [Fig. 5(a)], the boson population clearly behaves according to the standard quantum self-trapping. The population of the central site slowly decays. It exhibits damped oscillations and its first zero takes place for $t \approx 30\Phi^{-1}$. Then two wave packets are emitted on each side of the central site. They propagate very slowly so that almost all the initial energy is stored into the 12 sites surrounding

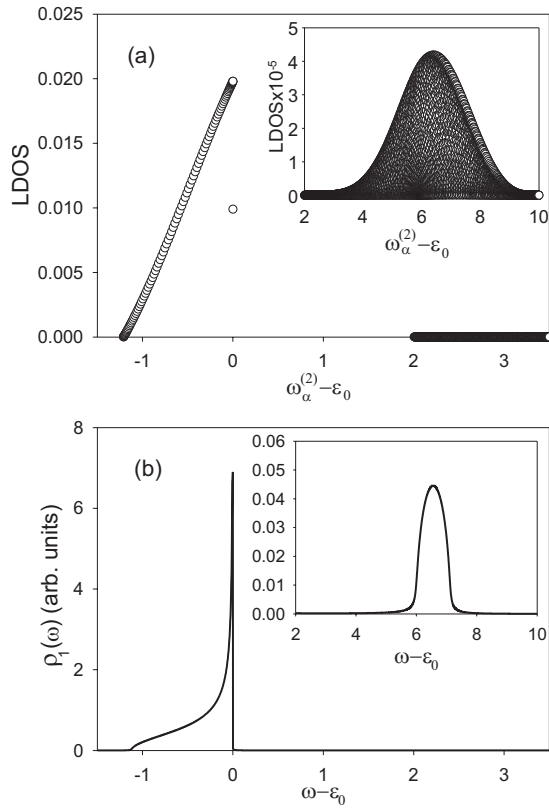


FIG. 4. (a) LDOS versus the eigenenergies for $\nu=2$, $A=3.0$, $N=61$, and $n_0=1$. (b) Theoretical LDOS.

$n_0=N/2$ at time $t=100\Phi^{-1}$. In marked contrast, when the three bosons are excited on a lattice side, Fig. 5(b) clearly shows that the main part of the energy stays localized on the excited site. Indeed, although the population of the side site slightly decreases in the short-time limit, it rapidly converges to an almost constant value equal to 2.76. In other words, 92% of the initial energy is stored in the side site initially excited.

The corresponding survival probability is shown in Fig. 6 for $A=1.0$ (dashed black line), $A=3.0$ (solid black line), and $A=5.0$ (solid gray line). As in Fig. 3(a), when $n_0=N/2$ [Fig. 6(a)], $P_{n_0}(t)$ shows damped oscillations, indicating that the energy is localized on the excited site over a finite time scale which increases with A . For $A=1, 3$, and 5 , its first zero is reached for $t=4.4\Phi^{-1}$, $30.0\Phi^{-1}$, and $81.0\Phi^{-1}$, respectively. Note that for $A=1$, a revival occurs around $t=60\Phi^{-1}$ due to the reflection over the lattice sides. As shown in Fig. 6(b), the survival probability of the side site $n_0=1$ exhibits a fully different behavior. During a transient regime whose duration increases with the nonlinearity, $P_1(t)$ decreases. Then, a permanent regime takes place in which $P_1(t)$ exhibits oscillations around an average value. Both the period and the amplitude of these oscillations decrease with A whereas the average value of the survival probability is enhanced by the nonlinearity. Consequently, for a sufficiently strong anharmonicity, $P_1(t)$ becomes almost constant in the permanent regime. These features clearly show that the energy is localized on the side site which has been excited.

For $\nu=3$, $A=3$, and $n_0=1$, the LDOS is illustrated in Fig. 7(a) in which the frequency reference is now denoted ϵ_0

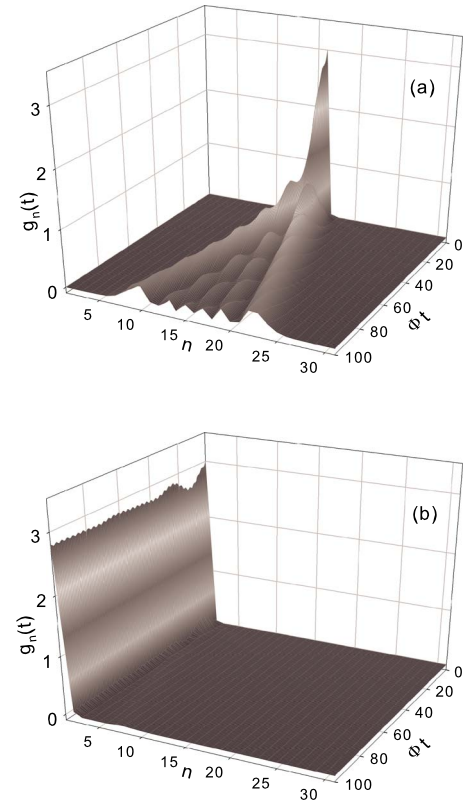


FIG. 5. (Color online) Space and time evolution of the boson population for $\nu=3$, $A=3.0$, and $N=31$ and for (a) $n_0=N/2$ and (b) $n_0=1$.

$=3\omega_0-6A$. To understand this figure, let us recall that the three-boson energy spectrum in a lattice with translational invariance exhibits two energy continua and three isolated bands (see Ref. 30). The high-frequency continuum charac-

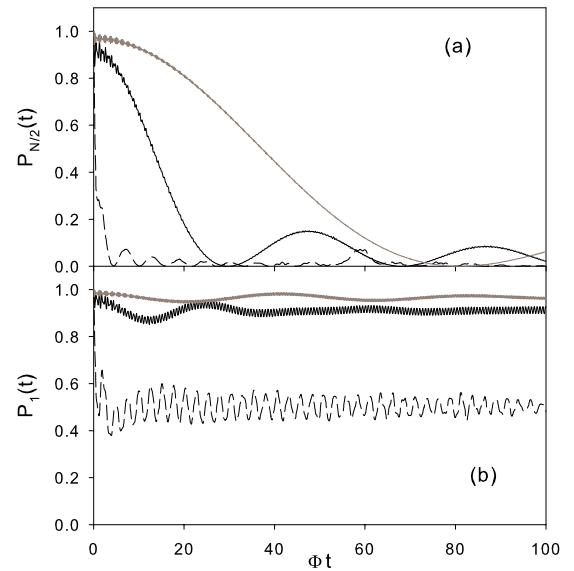


FIG. 6. (Color online) Time evolution of the survival probability for $\nu=3$ and for $A=1.0$ (dashed black line), $A=3.0$ (solid black line), and $A=5.0$ (solid gray line). (a) $n_0=N/2$ and (b) $n_0=1$.

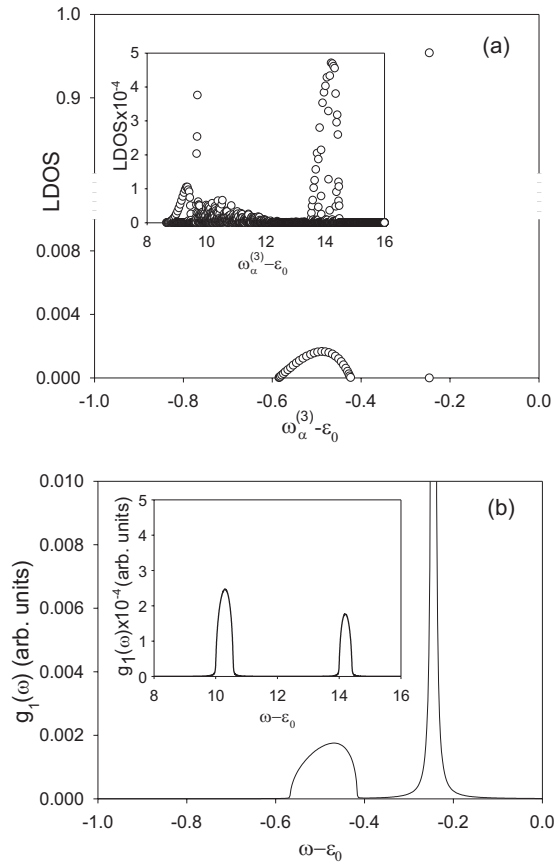


FIG. 7. (a) LDOS versus the eigenenergies for $v=3$, $A=3.0$, $N=31$, and $n_0=1$. (b) Theoretical LDOS.

terizes free states describing three independent bosons. The low-frequency continuum supports states in which two bosons are trapped on the same site, whereas the third boson propagates independently. By contrast, the isolated bands refer to bound states. The low-frequency band is the well-known soliton band which characterizes three bosons trapped on the same site and delocalized along the lattice. The two other bands, which lie, respectively, below and above the low-frequency continuum, describe bound states in which two bosons are trapped on a given site, whereas the third boson is trapped onto the corresponding nearest-neighbor sites. However, the two continua and the high-frequency bound-state bands overlap so that a single gap occurs which discriminates the soliton band from the rest of the spectrum.

As displayed in Fig. 7(a), the LDOS exhibits significant values in the soliton band which ranges between $\epsilon_0 - 0.585$ and $\epsilon_0 - 0.424$. In addition, it shows a peak at the frequency $\omega = \epsilon_0 - 0.247$ which lies outside the soliton band. A numerical analysis of the corresponding eigenvector has revealed that this peak characterizes a low-frequency localized state which refers to the localization of a three-boson bound state in the vicinity of one lattice side. By symmetry, the lattice supports a second bound state localized on the other side which produces a zero in the LDOS for the same frequency. Note that, in a general way, a finite-size lattice supports a left and a right low-frequency bound state localized on each side of the lattice. These states are not independent since they

interact through the core of the chain. The strength of this interaction depends on the overlap of their respective amplitudes which results from a competition between the lattice size and the localization length. Consequently, the true eigenstates are symmetric and antisymmetric superimpositions of the left and right localized bound states. However, in the present situation, the rather large value of the lattice size prevents any hybridization between the left and right localized states which correspond to the degenerated eigenstates obtained with the numerical diagonalization.

As shown in the inset of Fig. 7(a), a second peak occurs for $\omega = \epsilon_0 + 9.68$ but with a smaller intensity. This peak refers to a high-frequency localized state which describes two bosons trapped on a side site, the third boson being trapped in the corresponding nearest-neighbor sites. Consequently, in marked contrast with the cases $v=1$ and $v=2$, the way the energy is transferred strongly depends on the position of the excited site. When $n_0 = N/2$, only the soliton band is significantly excited so that transport is mediated by three-boson bound states which experience quantum self-trapping. By contrast, when $n_0 = 1$, the low-frequency localized states are preferentially excited. As a result, the main part of the energy stays localized on the side site. Note that the creation of three bosons on the side site also excites a high-frequency localized state, but to a lesser extent. Therefore, the boson population as well as the survival probability exhibits oscillations which originate in the superimposition of the two localized states as observed in Figs. 5 and 6.

The properties of the low-frequency localized state are summarized in Fig. 8 for $v=3$ and $N=31$. Open circles represent numerical calculations whereas solid lines describe theoretical results discussed in the next section. Note that the nonlinear parameter $\epsilon = 2A$ has been introduced for convenience. Let $\Psi_\alpha^{(3)}(n)$ denotes the projection of the localized wave function on the state characterizing three bosons on the site n . We have verified that $\sum_n |\Psi_\alpha^{(3)}(n)|^2$ is very close to unity once $A > 2$. For instance, for $A=3$ it is equal to 0.9796 and it reaches 0.9926 for $A=5$. Moreover, as illustrated in Fig. 8(a), the weight $|\Psi_\alpha^{(3)}(n=1)|^2$ increases with A to finally converge to unity. In other words, the numerical analysis of the localized state reveals that its decomposition on the number state basis mainly involves the configuration describing three bosons on the same site. The wave function is strongly localized on the side site and it develops an exponential shape defined as

$$\Psi_\alpha^{(3)}(n) \approx \Psi_\alpha^{(3)}(1)e^{-|n-1|/\xi}, \quad (7)$$

where ξ denotes the localization length. As shown in Fig. 8(b), ξ strongly depends on the nonlinearity since it drastically decreases with A . Finally, as displayed in Fig. 8(c), the frequency of the localized state increases with the nonlinearity. It converges to $\epsilon_0 = 3\omega_0 - 6A$ for strong A values—i.e., the value of the energy of three bosons on the same site.

IV. DISCUSSION

The numerical results have revealed that the dynamics of the finite-size lattice exhibits two regimes depending on the

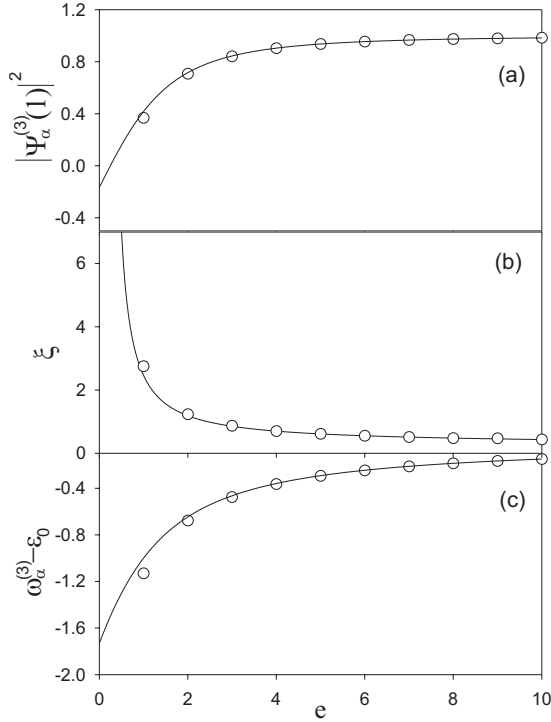


FIG. 8. Properties of the localized three-boson bound state. Open circles describe numerical calculations whereas solid lines refer to theoretical results. (a) Projection of the localized wave function on the state describing three bosons on the side site. (b) Localization length and (c) frequency of the localized state.

boson number. When $v=1$, the energy transport is mediated by extended states whatever the position of the excited site. The single boson delocalizes along the lattice according to a superimposition of plane waves whose average group velocity is about the hopping constant Φ . When $n_0=N/2$, two wave packets are emitted on each side of the central site whereas when $n_0=1$ a single wave packet propagates to reach the other side of the lattice. When $v=2$, similar features take place. Nevertheless, the creation of two bosons on a single site mainly excites the soliton band which describes two-boson bound states. According to the standard quantum self-trapping theory, these bound states delocalize along the lattice with an average group velocity of about Φ^2/A . The energy does not localize and bound states supply the energy transfer whatever the position of the excited site.

A fully different behavior occurs when $v=3$ since the way the energy delocalizes strongly depends on the position of the excited site. When $n_0=N/2$, only the soliton band is significantly excited so that the transport is mediated by three-boson bound states. These states experience quantum self-trapping and they take a very long time to tunnel from one site to another. The energy is thus localized around the central site over a finite time scale and it finally propagates along the lattice according to an average group velocity of about Φ^3/A^2 .

In a marked contrast, the creation of three bosons on a side site mainly excites a low-frequency localized state describing the trapping of three bosons in the surrounding of a lattice side. As a result, the main part of the energy stays

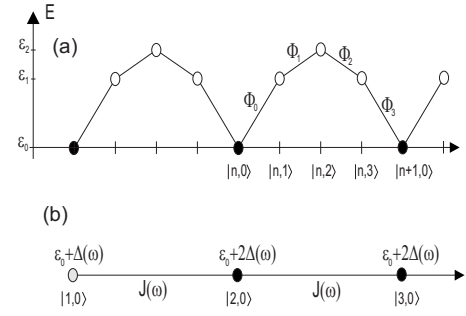


FIG. 9. Equivalent lattice model for $v=4$.

localized on the side site over an infinite timescale. This localization originates in the interplay between nonlinearity and symmetry breaking due to the presence of a lattice side. Therefore, the nonlinearity enhances the localization. It drastically reduces the localization length and favors the trapping of the three bosons on the side site. It controls the energy storage so that the larger the nonlinearity, the larger the amount of localized energy.

To interpret these observed features let us consider the model recently developed in Ref. 30. This model is based on the numerical observation that, due to the initial creation of v bosons on a single site, the lattice dynamics is confined in a restriction of the v -boson subspace E_v . The dimension of the problem is thus reduced so that the model provides a simple view of the dynamics in which bound states play the central role. Nevertheless, since the original model was introduced to characterize a lattice with translational invariance, it must be modified to account for the symmetry breaking. To proceed, we shall restrict our attention to a semi-infinite lattice exhibiting a single side. As shown in the following text, the presence of a single side is sufficient to clearly understand the way localized states occur in the finite-size lattice.

A. Equivalent lattice model

According to our previous model,³⁰ the dynamics in E_v is relatively well described by restricting the number state basis to a set of relevant vectors. A relevant vector $|n,p\rangle$ characterizes $v-p$ quanta of the n th site and p quanta of the site $n+1$. For $n \geq 1$, the representation of H in the relevant basis yields a tight-binding model on the semi-infinite lattice displayed in Fig. 9(a). Each lattice site supports the state $|n,p\rangle$ whose energy is $\epsilon_p = \epsilon_0 + p(v-p)\epsilon$, where $\epsilon = 2A$. Note that $\epsilon_0 = v\omega_0 - v(v-1)A$ will be used as the origin of the energy—i.e., $\epsilon_0 = 0$. Nearest-neighbor sites are coupled to each other through a generalized hopping constant $\Phi_p = \sqrt{(p+1)(v-p)}\Phi$ which connects $|n,p\rangle$ and $|n,p+1\rangle$ for $p = 0, \dots, v-2$. By symmetry, $|n,v-1\rangle$ and $|n+1,0\rangle$ interacts through $\Phi_0 = \sqrt{v}\Phi$. As shown in Fig. 9(a), the lattice can be partitioned into two sublattices. The first sublattice is formed by the states $|n,0\rangle$ ($n \geq 1$). For each n value, the second sublattice involves the so-called modified dimer formed by the $v-1$ coupled states $|n,p\rangle$ ($p = 1, \dots, v-1$) whose Hamiltonian is denoted \mathcal{H} .

Consequently, when v bosons are created on the site n_0 , the dynamics of the nonlinear lattice is formally equivalent

to that of a fictitious particle moving on the lattice shown in Fig. 9(a). This equivalence allows us to evaluate analytically the LDOS and the survival probability giving rise to a complete understanding of the lattice dynamics.

B. Green function calculation

According to the standard definition used in condensed matter physics, the LDOS, Eq. (6), is expressed as

$$\rho_{n_0}(\omega) = -\frac{1}{\pi} \text{Im} G_{n_0 n_0}(\omega + i0^+), \quad (8)$$

where $G_{nn'}(\omega)$ denotes the restriction of the lattice Green operator to the first sublattice involving the states $|n, 0\rangle$. By applying a standard projection method, it is defined as (see, for instance, Ref. 50)

$$G(\omega) = [\omega - \Sigma(\omega)]^{-1}. \quad (9)$$

In Eq. (9), the nonvanishing elements of the self-energy operator $\Sigma(\omega)$ are expressed as

$$\Sigma_{nn'}(\omega) = \delta_{n,n'}(2 - \delta_{n,1})\Delta(\omega) + (\delta_{n,n'+1} + \delta_{n,n'-1})J(\omega), \quad (10)$$

where both $\Delta(\omega)$ and $J(\omega)$ are defined in terms of the modified dimer Green function $\mathcal{G}(\omega) = (\omega - \mathcal{H})^{-1}$ as

$$\begin{aligned} \Delta(\omega) &= \Phi_0^2 \mathcal{G}_{1,1}(\omega), \\ J(\omega) &= \Phi_0^2 \mathcal{G}_{1,v-1}(\omega). \end{aligned} \quad (11)$$

The projection $G(\omega)$ is equivalent to the Green function of a semi-infinite lattice which exhibits a defect. As illustrated in Fig. 9(b), each site n of this lattice supports the state $|n, 0\rangle$. Therefore, nearest-neighbor sites interact through the effective hopping constant $J(\omega)$ which describes the coupling between $|n, 0\rangle$ and $|n+1, 0\rangle$ mediated by the n th modified dimer. In addition, for $n > 1$, the self-energy $2\Delta(\omega)$ of the n th site accounts for the renormalization of the energy of the state $|n, 0\rangle$ due to its interaction with its two nearest-neighbor modified dimers. However, since the site $n=1$ is coupled to a single modified dimer, it is characterized by a reduced self-energy equal to $\Delta(\omega)$, only.

According to the general procedure introduced by Dobrzynski⁵¹ to calculate the response function of composite materials, the Green function of the semi-infinite lattice is written as

$$G_{nn'}(\omega) = G_{00}^\infty(\omega) \left[t(\omega)^{|n-n'|} - \frac{\Delta(\omega) + J(\omega)t(\omega)}{\Delta(\omega) + J(\omega)t(\omega)^{-1}} t(\omega)^{n+n'-2} \right], \quad (12)$$

where the Green function of an infinite chain is defined as

$$G_{nn'}^\infty(\omega) = \frac{t(\omega)^{|n-n'|}}{J(\omega)[t(\omega)^{-1} - t(\omega)]}. \quad (13)$$

In Eqs. (12) and (13), the parameter $t(\omega)$ is defined as

$$t(\omega) = \frac{\omega - 2\Delta(\omega)}{2J(\omega)} \pm i \sqrt{1 - \left(\frac{\omega - 2\Delta(\omega)}{2J(\omega)} \right)^2}, \quad (14)$$

where the sign \pm is chosen to ensure the regular behavior of the Green function when $|n-n'| \rightarrow \infty$ and $\omega \equiv \omega + i0^+$.

Far from the lattice side, Eq. (12) reveals that $G(\omega)$ tends to $G^\infty(\omega)$. Consequently, the LDOS is equal to that of an infinite lattice as

$$\rho_\infty(\omega) = \frac{1}{\pi} \frac{1}{\sqrt{4J^2(\omega) - [\omega - 2\Delta(\omega)]^2}}. \quad (15)$$

It takes nonvanishing values in the frequency range specified by the inequality $|\omega - 2\Delta(\omega)|/2J(\omega) < 1$. This range defines the allowed energy bands describing the delocalization of the fictitious particle on the equivalent lattice—i.e., the bound-state energy bands (see Ref. 30).

By contrast, the projection of the Green function on the lattice side reduces to

$$G_{11}(\omega) = \frac{1}{\Delta(\omega) + J(\omega)t(\omega)^{-1}}, \quad (16)$$

so that the corresponding LDOS is defined as

$$\rho_1(\omega) = -\frac{1}{\pi} \text{Im} \frac{1}{\Delta(\omega) + J(\omega)t(\omega)^{-1}}. \quad (17)$$

Due to the presence of a defect on the site $n=1$, we expect the occurrence of a localized state whose frequency corresponds to a discrete pole of $G_{11}(\omega)$ [Eq. (16)]. If a pole occurs at frequency Ω , $t(\Omega)$ scales as $\exp[-1/\xi(\Omega)]$ to ensure the localized behavior of the Green function. The localization length $\xi(\Omega)$ is thus written as

$$\xi(\Omega) = \frac{1}{\ln|\Delta(\Omega)/J(\Omega)|}. \quad (18)$$

Therefore, Eqs. (16)–(18) show that the occurrence of a localized state requires $|\Delta(\omega)/J(\omega)| > 1$. The localization results from competition between the strength of the defect, characterized by the parameter $\Delta(\omega)$, and the hopping constant $J(\omega)$, which enhances the delocalization. As shown in Eq. (11), these two parameters depend on the properties of the modified dimer which are very sensitive to both the boson number and the nonlinearity. We thus expect that the occurrence of localized states strongly depends on these two ingredients. These features are first illustrated in the following sections for the three simple situations $v=1$, $v=2$, and $v=3$. Then, a general discussion is given for larger v values.

C. Application to $v=1$

The situation $v=1$ is a very special case since the equivalent lattice do not exhibit any modified dimer. The states $|n, 0\rangle$ are coupled to each other directly so that $\Delta(\omega)=0$ and $J(\omega)=\Phi$. Equations (16)–(18) clearly show that there is no localized state and the LDOS, Eqs. (15) and (17), are rewritten as

$$\rho_{\infty}(\omega) = \frac{1}{2\pi\Phi} \frac{1}{\sqrt{1 - (\omega/2\Phi)^2}},$$

$$\rho_1(\omega) = \frac{1}{\pi\Phi} \sqrt{1 - (\omega/2\Phi)^2}. \quad (19)$$

Whatever the position of the excited site, the two LDOS define a single energy band $-2\Phi < \omega < 2\Phi$. As in a lattice with translational invariance, this band describes extended states corresponding to superimpositions of incident and reflected plane waves. The LDOS $g_{\infty}(\omega)$ exhibits two divergences located on the band edges, whereas $g_1(\omega)$ vanishes when $\omega = \pm 2\Phi$.

These features indicate that the time evolution of the survival probability slightly depends on the position of the excited site as

$$P_n(t) = |J_0(2\Phi t) - (-1)^n J_{2n}(2\Phi t)|^2, \quad (20)$$

where $J_n(z)$ is a Bessel function of the first kind and where $P_{\infty}(t) = J_0^2(2\Phi t)$ denotes the response to an excitation far from the lattice side. In the very-short-time limit, $P_{\infty}(t)$ decays more rapidly than $P_1(t)$. Then, in perfect agreement with the numerical results displayed in Fig. 1, $P_{\infty}(t)$ supports damped oscillations in the long-time limit. These oscillations decrease according to time and the survival probability scales as the invert law $P_{\infty}(t) \propto 1/t$. In marked contrast, $P_1(t)$ does not show any significant oscillations and it decays according to the invert power law $P_{\infty}(t) \propto 1/t^3$.

Therefore, whatever the position of the excited site, the boson delocalizes along the lattice according to extended states. Far from the lattice side, its coherent motion leads to periodic returns to the excited site but with decreasing probability amplitude. This effect does not occur when $n_0=1$ since the boson rapidly leaves the lattice side to propagate toward the core of the lattice.

D. Application to $v=2$

When $v=2$, a modified dimer involves a single state $|n, 1\rangle$ whose energy is $\epsilon_1 = \epsilon$. Consequently, $\Delta(\omega) = J(\omega) = 2\Phi^2/(\omega - \epsilon)$ so that the strength of the defect is not large enough to produce a localized state. The Green function does not exhibit any discrete pole, and the LDOS are defined as

$$\rho_{\infty}(\omega) = \frac{1}{\pi} \sqrt{\frac{-(\omega - \epsilon_1)}{\omega(\omega - \omega_+)(\omega - \omega_-)}},$$

$$\rho_1(\omega) = \frac{1}{4\pi\Phi^2} \sqrt{\frac{-(\omega - \epsilon_1)(\omega - \omega_+)(\omega - \omega_-)}{\omega}}, \quad (21)$$

where $\omega_{\pm} = \epsilon/2 \pm \sqrt{\epsilon^2/4 + 8\Phi^2}$.

When $\epsilon \gg \Phi$, the LDOS show two well-separated bands. The low-frequency band, whose energy ranges between ω_- and 0, characterizes the delocalization of the fictitious particle over the different states $|n, 0\rangle$. It refers to the soliton band describing two bosons trapped on the same site and delocalized along the lattice. By contrast, the second band accounts for the delocalization of the particle over the states

$|n, 1\rangle$. It thus describes bosons trapped onto two nearest-neighbor sites. Equations (21) reveal that the two LDOS take significant values in the frequency range of the soliton band. $g_{\infty}(\omega)$ exhibits two divergences located on the band edges whereas, as illustrated in Fig. 4(b) for $A=3$, $g_1(\omega)$ vanishes when $\omega = \omega_-$ and it diverges when $\omega = 0$. In close agreement with the numerical results [see Fig. 4(a)], the excitation of the soliton band due to the creation of two bosons on the lattice side is not symmetric and a key role is played by bound states lying close to the high-frequency edge of the band.

Consequently, the soliton band controls the main part of the dynamics whatever the position of the excited side, and, in the limit $\epsilon \gg \Phi$, it is straightforward to show that the survival probabilities behave as

$$P_n(t) \approx J_0^2\left(\frac{4\Phi^2 t}{\epsilon}\right) + J_{2n-1}^2\left(\frac{4\Phi^2 t}{\epsilon}\right). \quad (22)$$

According to the standard quantum self-trapping, $P_{\infty}(t)$ exhibits damped oscillations which characterize the delocalization of the two trapped bosons. It slowly decays and it reaches its first zero for $t = 2.4\epsilon/4\Phi^2$. When $A=3$, this value is equal to $3.6\Phi^{-1}$, in close agreement with the numerical results about $4\Phi^{-1}$ (see Fig. 3). As for $v=1$, the survival probability scales as $P_{\infty}(t) \propto 1/t$ in the long-time limit. However, in marked contrast with the case $v=1$, $P_{\infty}(t)$ and $P_1(t)$ evolve over a similar time scale. Indeed, when the side site is excited the energy is still transported by two-boson bound states. Although $P_1(t)$ does not show any significant oscillations, it does not vanish rapidly. It scales as $P_1(t) \propto 1/t$ so that the nonlinearity prevents the two trapped bosons to leave rapidly the side site.

E. Application to $v=3$

When $v=3$, a modified dimer involves the two states $|n, 1\rangle$ and $|n, 2\rangle$. They have the same energy 2ϵ and they strongly hybridize due to the coupling $\Phi_1 = 2\Phi$. Therefore, the eigenstates of a modified dimer are symmetric and anti-symmetric superimpositions of $|n, 1\rangle$ and $|n, 2\rangle$ whose eigenenergies are $\epsilon_{\pm} = 2\epsilon \pm 2\Phi$. The dynamical parameters $\Delta(\omega)$ and $J(\omega)$ are thus defined as [Eq. (11)]

$$\Delta(\omega) = \frac{3\Phi^2}{2} \left(\frac{1}{\omega - \epsilon_+} + \frac{1}{\omega - \epsilon_-} \right),$$

$$J(\omega) = \frac{3\Phi^2}{2} \left(\frac{1}{\omega - \epsilon_+} - \frac{1}{\omega - \epsilon_-} \right). \quad (23)$$

When the three bosons are created far from the lattice side, they behave as in a lattice with translational invariance. The LDOS is thus expressed as

$$\rho_{\infty}(\omega) = \frac{1}{\pi} \sqrt{\frac{-(\omega - \epsilon_+)(\omega - \epsilon_-)}{(\omega - \omega_1)(\omega - \omega_2)(\omega - \omega_3)(\omega - \omega_4)}}, \quad (24)$$

where the four poles, given by Eq. (22) in Ref. 30, are expressed in the limit $\epsilon \gg \Phi$ as

$$\begin{aligned}
\omega_1 &\approx -3\frac{\Phi^2}{\epsilon} - 3\frac{\Phi^3}{\epsilon^2}, \\
\omega_2 &\approx -3\frac{\Phi^2}{\epsilon} + 3\frac{\Phi^3}{\epsilon^2}, \\
\omega_3 &\approx 2\epsilon - 2\Phi + 3\frac{\Phi^2}{\epsilon} + 3\frac{\Phi^3}{\epsilon^2}, \\
\omega_4 &\approx 2\epsilon + 2\Phi + 3\frac{\Phi^2}{\epsilon} - 3\frac{\Phi^3}{\epsilon^2}.
\end{aligned} \tag{25}$$

For strong ϵ values, the LDOS shows three bands well separated. The low-frequency band, which ranges between ω_1 and ω_2 , describes the delocalization of the fictitious particle over the different states $|n, 0\rangle$. It thus corresponds to the soliton band whose the LDOS exhibits two divergences at the band edges. The resulting bandwidth is thus about $6\Phi^3/\epsilon^2$. By contrast, the band just above the soliton band ($\epsilon_- < \omega < \omega_3$) refers to bound states formed by the antisymmetric superimposition of the states $|n, 1\rangle$ and $|n, 2\rangle$, whereas the high-frequency band ($\epsilon_+ < \omega < \omega_4$) characterizes bound states involving their symmetric superimposition. The LDOS connected to these two bands shows a single divergence and a single zero.

Since only the soliton band is significantly excited, it controls the main part of the dynamics. The survival probability is thus approximately expressed as

$$P_\infty(t) \approx J_0^2 \left(\frac{3\Phi^3 t}{\epsilon^2} \right). \tag{26}$$

It exhibits a rather slow dynamics and decreases over a time scale typically of about $t = 2.40\epsilon^2/3\Phi^3$. When $A=3$, this time is equal to $28.8\Phi^{-1}$, in close agreement with the numerical results $30\Phi^{-1}$ [see Fig. 6(a)].

When the three bosons are created on the lattice side, two situations occur depending on whether the frequency lies in the previous energy bands or not. Indeed, when ω belongs to the energy bands, the Green function describes extended bound states and the LDOS is expressed as

$$\rho_1(\omega) = \frac{\sqrt{-(\omega - \epsilon_+)(\omega - \epsilon_-) \prod_{i=1}^4 (\omega - \omega_i)}}{6\pi\Phi^2(\omega - \Omega_-)(\omega - \Omega_+)}, \tag{27}$$

where $\Omega_\pm = \epsilon \pm \sqrt{\epsilon^2 + 3\Phi^2}$. Note that $\omega_2 < \Omega_- < \epsilon_-$ and $\omega_3 < \Omega_+ < \epsilon_+$ in the strong- ϵ limit. As illustrated in Fig. 7(b) for $A=3$, the LDOS does not show any divergence. It takes rather small values and it vanishes at each band edge. These features clearly indicate that the contribution of the bound state bands to the survival probability is very small so that extended states do not control the behavior of the three bosons.

In fact, a detailed analysis of Eqs. (16)–(18) reveals that the Green function exhibits a discrete pole whose frequency is equal to $\Omega_- = \epsilon - \sqrt{\epsilon^2 + 3\Phi^2}$. This pole lies just above the soliton band and it refers to a localized state in the equivalent lattice. It describes three trapped bosons which behave as a single particle whose wave function is strongly localized

near the lattice side. Because $J(\Omega_-) > 0$ and $\Delta(\Omega_-) < 0$, the regularity of the Green function is ensured when $t(\Omega_-) = (\Omega_- - 2\Delta)/2J - \sqrt{[(\Omega_- - 2\Delta)/2J]^2 - 1}$. This parameter scales as $t(\Omega_-) = \exp(-1/\xi)$ so that the wave function is exponentially localized according to the localization length ξ defined as [see Eq. (18)]

$$\xi^{-1} = \ln \frac{\epsilon + \sqrt{\epsilon^2 + 3\Phi^2}}{2\Phi}. \tag{28}$$

The localized state produces a peak in the local density of states outside the allowed energy band. The corresponding LDOS is written as

$$\rho_1(\omega) = S(\Omega_-) \delta(\omega - \Omega_-), \tag{29}$$

where $S(\Omega_-)$ defines the weight of the state $|1, 0\rangle$ in the localized state as

$$S(\Omega_-) = -\frac{\Omega_-(\epsilon_+ - \Omega_-)(\epsilon_- - \Omega_-)}{3\Phi^2(\Omega_+ - \Omega_-)}. \tag{30}$$

As displayed in Fig. 7(b) for $A=3$, the peak in the LDOS is located at the frequency $\Omega_- = -0.2449$, in perfect agreement with the numerical value of the frequency peak equal to -0.245 . In addition, as illustrated in Fig. 8, the properties of the localized states versus the nonlinear parameter ϵ allows us to recover the numerical results. The weight of $|1, 0\rangle$ in the localized state is enhanced by the nonlinearity and it scales as $S(\Omega_-) \approx 1 - 7\Phi^2/4\epsilon^2$ in the strong- ϵ limit [Fig. 8(a)]. The localization length decreases with the nonlinearity and it tends to zero according to the invert logarithm law $\xi \approx 1/\ln(\epsilon/\Phi)$ [Fig. 8(b)]. Finally, as shown in Fig. 8(c), the frequency of the localized state increases with the nonlinearity. It scales as $\Omega_- \approx -3\Phi^2/2\epsilon$ and it converges to zero—i.e., the value of the self-energy of the side site $|1, 0\rangle$.

Consequently, the creation of three bosons on the side site mainly excites the localized state. The corresponding survival amplitude is thus the sum of two contributions. The first contribution characterizes the very small response of the soliton band whereas the second contribution, equal to $S(\Omega_-)\exp(-i\Omega_-t)$, accounts for the influence of the localized state. Therefore, after a time scale of about $\epsilon^2/3\Phi^3$, the contribution of the continuous soliton band has disappeared so that the survival probability becomes constant and equal to $P_1(t) = S(\Omega_-)^2$. In the strong- ϵ limit, the main part of the deposited energy is thus stored in the localized state which basically refers to three bosons trapped on the side site. In marked contrast with the standard quantum self-trapping, the localization takes place over an infinite time scale.

F. Application to large v values

As shown in the previous section for $v=3$, the equivalent lattice model gives theoretical results in a very good agreement with the numerical simulations. This feature allows us to generalize this model to larger v values for which exact simulations cannot be done easily due to the exponential increase of the Hilbert-space dimension. In that context, although a numerical study of this model can be realized straightforwardly, we present analytical results obtained by

performing suitable approximations in the limit of a strong nonlinearity.

When $\epsilon \gg \Phi$, the states $|n, 0\rangle$ are strongly nonresonant with modified dimers. Therefore, they tend to hybridize to each other to produce the soliton band which describes v bosons trapped on the same site. The bosons behave as a single particle on a semi-infinite lattice whose dynamics is governed by a tight-binding model involving the parameters $\Delta(\omega)$ and $J(\omega)$. As shown in Eq. (11), these parameters are defined in terms of the restriction of the Green function of a modified dimer to the states $|n, 1\rangle$ and $|n, v-1\rangle$. In the strong- ϵ limit, this restriction can be evaluated approximately by performing a perturbative expansion of the Green function.

Therefore, in perfect analogy with the case $v=3$, a modified dimer can be viewed as a two-level system formed by $|n, 1\rangle$ and $|n, v-1\rangle$. These states have the same energy $\hat{\epsilon}_1$ and they hybridize according to a coupling μ_v . In addition to $\epsilon_1=(v-1)\epsilon$, the energy $\hat{\epsilon}_1$ of $|n, 1\rangle$ (respectively $|n, v-1\rangle$) includes the lowest-order correction due to its coupling with the remaining states of a modified dimer. Similarly, μ_v describes the effective interaction between $|n, 1\rangle$ and $|n, v-1\rangle$ mediated by the remaining states $|n, p\rangle$ ($p=2, \dots, v-2$). These two parameters are thus defined as

$$\begin{aligned}\hat{\epsilon}_1 &\approx (v-1)\epsilon - \frac{v-1}{v-2} \frac{\Phi^2}{\epsilon}, \\ \mu_v &\approx (-1)^{v-1} \frac{v-1}{(v-2)!} \frac{\Phi^{v-2}}{\epsilon^{v-3}}.\end{aligned}\quad (31)$$

Consequently, the low-energy eigenstates of a modified dimer are symmetric and antisymmetric superimpositions of $|n, 1\rangle$ and $|n, v-1\rangle$ whose eigenenergies are $\hat{\epsilon}_\pm = \hat{\epsilon}_1 \pm |\mu_v|$. In that context, the dynamical parameters $\Delta(\omega)$ and $J(\omega)$ are written as

$$\begin{aligned}\Delta(\omega) &= \frac{v\Phi^2}{2} \left(\frac{1}{\omega - \hat{\epsilon}_+} + \frac{1}{\omega - \hat{\epsilon}_-} \right), \\ J(\omega) &= (-1)^{v-1} \frac{v\Phi^2}{2} \left(\frac{1}{\omega - \hat{\epsilon}_+} - \frac{1}{\omega - \hat{\epsilon}_-} \right).\end{aligned}\quad (32)$$

Note that, when $v=3$, Eq. (32) is still exact provided that $\hat{\epsilon}_1=2\epsilon$.

When v bosons are created far from the lattice side, they behave as in a lattice with translational invariance so that the LDOS is expressed as

$$\rho_\infty(\omega) = \frac{1}{\pi} \sqrt{\frac{-(\omega - \hat{\epsilon}_+)(\omega - \hat{\epsilon}_-)}{(\omega - \omega_1)(\omega - \omega_2)(\omega - \omega_3)(\omega - \omega_4)}}, \quad (33)$$

where the four poles are defined as

$$\begin{aligned}\omega_1 &\approx -\omega_s - 2\Phi_s, \\ \omega_2 &\approx -\omega_s + 2\Phi_s, \\ \omega_3 &\approx \hat{\epsilon}_1 - |\mu_v| + \omega_s + 2\Phi_s, \\ \omega_4 &\approx \hat{\epsilon}_1 + |\mu_v| + \omega_s - 2\Phi_s.\end{aligned}\quad (34)$$

In Eq. (34), $\omega_s=2v\Phi^2/(v-1)\epsilon$ and Φ_s stands for the effective hopping constant for v boson bound states as^{26,27,30}

$$\Phi_s = \frac{v\Phi^v}{(v-1)! \epsilon^{v-1}}. \quad (35)$$

Although the LDOS exhibits three well-separated bands, it takes significant values in the low-frequency band, only. This band, which ranges between ω_1 and ω_2 , describes the delocalization of the fictitious particle along the states $|n, 0\rangle$. It refers to the soliton band in which the LDOS exhibits two divergences at the edges. The soliton band is rather narrow and the resulting bandwidth, about $4\Phi_s$, decreases with both the boson number and the nonlinearity. Since the soliton band controls the main part of the dynamics, the survival probability behaves as

$$P_\infty(t) \approx J_0^2(2\Phi_s t). \quad (36)$$

According to the standard quantum self-trapping, it exhibits a very slow dynamics and it decays over a time scale typically of about ϵ^{v-1}/Φ^v .

When v bosons are created on the lattice side, the study of Eq. (16) reveals that for large v values, the lattice Green function supports a discrete pole. The corresponding frequency, equal to $\hat{\Omega}_- = \hat{\epsilon}_1/2 - \sqrt{(\hat{\epsilon}_1/2)^2 + v\Phi^2}$, scales as

$$\hat{\Omega}_- \approx -\frac{v\Phi^2}{(v-1)\epsilon}. \quad (37)$$

The discrete pole describes a localized state in which v trapped bosons behave as a single particle localized near the lattice side. From Eq. (18), it is straightforward to show that the corresponding localization length is written as ($\epsilon \gg \Phi$)

$$\xi^{-1} = \ln \left[(v-2)! \left(\frac{\epsilon}{\Phi} \right)^{v-2} \right]. \quad (38)$$

Equation (38) reveals that ξ exhibits a logarithmic divergence for $v=2$. Indeed, the position of the pole strongly depends on the boson number and it lies outside the soliton band if $\hat{\Omega}_- > \omega_1$. When $\epsilon \gg \Phi$, this condition is satisfied when $(v-2)! > 2(\Phi/\epsilon)^{v-2}$. Therefore, the occurrence of a localized state requires a boson number larger than 2, in perfect agreement with the numerical observations.

Consequently, the localized state yields a peak in the LDOS which is expressed as

$$\rho_1(\omega) = S(\hat{\Omega}_-) \delta(\omega - \hat{\Omega}_-), \quad (39)$$

where $S(\hat{\Omega}_-)$, the weight of the state $|1, 0\rangle$ in the localized state, behaves as

$$S(\hat{\Omega}_-) \approx 1 - \left(\frac{v}{(v-1)^2} + \delta_{v3} \right) \left(\frac{\Phi}{\epsilon} \right)^2. \quad (40)$$

Equation (40) clearly shows that the creation of v bosons on the lattice side mainly excites the localized state whose local nature is strongly enhanced by both nonlinearity and boson number. The survival probability converges to a constant value $P_1(t) \approx S(\hat{\Omega}_-)^2$ which indicates that the main part of the

deposited energy is trapped on the lattice side over an infinite timescale.

According to Eqs. (37)–(40), a large boson number enhances the localization. It drastically reduces the localization length and it favors the trapping of the v bosons on the side site. It controls the energy storage so that the larger the boson number, the larger the amount of energy trapped in the localized state. In fact, the influence of the boson number originates in competition between the strength of the defect $\Delta(\omega)$ and the effective hopping constant $J(\omega)$. For strong ϵ values, the very small value of the soliton bandwidth allows one to neglect the frequency dependence of these two parameters. They thus typically scale as $\Delta(0) \approx v\Phi^2/(v-1)\epsilon$ and $J(0) \approx \Phi_s$, respectively [see Eqs. (32) and (35)]. Therefore, for large v values, $\Delta(0)$ converges to Φ^2/ϵ whereas $J(0)$ decreases exponentially. The effective hopping constant is thus more sensitive to the boson number than the frequency shift. Consequently, the localization does not result from an enhancement of the strength of the defect but it originates in a strong decay of the ability of the bound states to delocalize toward the core of the lattice.

V. CONCLUSION

In the present paper, a Bose version of the Hubbard model has been used to study the dynamics of multiboson bound states in a finite-size lattice. It has been shown that the interplay between the symmetry breaking and the nonlinearity is responsible for the occurrence of a surprising effect since bound states may localize on each lattice side. However, both numerical calculations and theoretical analysis have revealed that the localization takes place for a boson number greater than a critical value equal to $v=2$.

Indeed, when $v=1$, the nonlinearity does not modify the boson dynamics and the energy is transported by extended states whatever the position of the excited site. When $v=2$, similar features have been observed. Nevertheless, the nonlinearity now plays a key role since the creation of two bosons mainly excites the soliton band. The energy does not localize and bound states supply the energy transfer whatever the position of the excited site.

For $v=3$, our numerical calculations have revealed the occurrence of a fully different behavior. Indeed, when the three bosons are created far from the lattice side, only the soliton band is significantly excited so that the transport is

mediated by three-boson bound states. These states experience the quantum self-trapping and they take a very long time to tunnel from one site to another. The energy is thus localized around the central site over a finite time scale and it finally propagates along the lattice. By contrast, the creation of three bosons on a side site mainly excites a low-frequency localized state describing the trapping of three bosons in the surrounding of a lattice side. As a result, the main part of the energy stays localized on the side site over an infinite timescale.

Based on analytical calculations, it has been shown that v trapped bosons experience a different self-energy whether they lie on a side site or on a core site. This energy difference yields a defect on a lattice side which is responsible for the occurrence of a localized state for $v > 2$. Nevertheless, the localization does not result from an enhancement of the strength of the defect but it originates in a strong decay of the ability of the bound states to propagate toward the core of the lattice. Indeed, the bound-state effective hopping constant is very sensitive to both the boson number and the nonlinearity which drastically enhance the localization. The boson number and the nonlinearity strongly reduce the localization length and they favor the trapping of the bosons on the side site. They control the energy storage so that the larger the boson number and nonlinearity, the larger the amount of localized energy.

To conclude, let us mention that the previous results allow us to point out both the analogies and the differences between quantum and classical nonlinear lattices. Indeed, it has been shown recently that a semi-infinite lattice, whose dynamics is described by the DNLS equation, exhibits nonlinear surface waves (see, for instance, Refs. 43–49). Similarly to the features reported in the present work, these localized self-trapped states occur above a certain power threshold proportional to the norm of the classical field. Nevertheless, since the norm is the classical counterpart of the average boson number, these results suggest that localized states can occur even if $v \leq 2$, provided that the nonlinearity is sufficiently strong. In marked contrast, our calculations show the existence of a critical boson number $v=2$. This purely quantum effect, which has no classical counterpart, seems to point out the inability of the DNLS equation to correctly describe the dynamics of the Bose-Hubbard model involving a rather small boson number. Nevertheless, this question remains an open question which requires further investigation.

*vincent.pouthier@univ-fcomte.fr

¹A. S. Davydov and N. I. Kislukha, Phys. Status Solidi B **59**, 465 (1973); Zh. Eksp. Teor. Fiz. **71**, 1090 (1976) [Sov. Phys. JETP **44**, 571 (1976)].

²A. C. Scott, Phys. Rep. **217**, 1 (1992).

³P. L. Christiansen and A. C. Scott, *Davydov's Soliton Revisited* (Plenum, New York, 1990).

⁴A. C. Scott and J. C. Eilbeck, Chem. Phys. Lett. **132**, 23 (1986).

⁵D. N. Christodoulides and R. I. Joseph, Opt. Lett. **13**, 794 (1988).

⁶A. Trombettoni and A. Smerzi, Phys. Rev. Lett. **86**, 2353 (2001).

⁷R. A. Vicencio, J. Brand, and S. Flach, Phys. Rev. Lett. **98**, 184102 (2007).

⁸J. C. Eilbeck, P. S. Lomdahl, and A. C. Scott, Phys. Rev. B **30**, 4703 (1984).

⁹J. C. Eilbeck, P. S. Lomdahl, and A. C. Scott, Physica D **16**, 318 (1985).

¹⁰A. J. Sievers and S. Takeno, Phys. Rev. Lett. **61**, 970 (1988).

¹¹S. Aubry, Physica D **103**, 201 (1997).

- ¹²S. Flach and C. R. Willis, *Phys. Rep.* **295**, 181 (1998).
¹³R. S. MacKay, *Physica A* **288**, 174 (2000).
¹⁴V. Fleurov, *Chaos* **13**, 676 (2003).
¹⁵J. C. Kimball, C. Y. Fong, and Y. R. Shen, *Phys. Rev. B* **23**, 4946 (1981).
¹⁶F. Bogani, G. Cardini, V. Schettino, and P. L. Tasselli, *Phys. Rev. B* **42**, 2307 (1990).
¹⁷V. Pouthier, *J. Chem. Phys.* **118**, 9364 (2003).
¹⁸V. Pouthier, *Phys. Rev. E* **68**, 021909 (2003).
¹⁹V. Pouthier and C. Falvo, *Phys. Rev. E* **69**, 041906 (2004).
²⁰C. Falvo and V. Pouthier, *J. Chem. Phys.* **123**, 184710 (2005).
²¹G. Kalosakas and A. R. Bishop, *Phys. Rev. A* **65**, 043616 (2002).
²²G. Kalosakas, A. R. Bishop, and V. M. Kenkre, *Phys. Rev. A* **68**, 023602 (2003).
²³G. Kalosakas, A. R. Bishop, and V. M. Kenkre, *J. Phys. B* **36**, 3233 (2003).
²⁴V. Z. Enol'skii, M. Salerno, A. C. Scott, and J. C. Eilbeck, *Physica D* **59**, 1 (1992).
²⁵E. Wright, J. C. Eilbeck, M. H. Hays, P. D. Miller, and A. C. Scott, *Physica D* **69**, 18 (1993).
²⁶L. Bernstein, J. C. Eilbeck, and A. C. Scott, *Nonlinearity* **3**, 293 (1990).
²⁷A. C. Scott, J. C. Eilbeck, and H. Gilhoj, *Physica D* **78**, 194 (1994).
²⁸J. Dorignac, J. C. Eilbeck, M. Salerno, and A. C. Scott, *Phys. Rev. Lett.* **93**, 025504 (2004).
²⁹L. Proville, *Phys. Rev. B* **71**, 104306 (2005).
³⁰C. Falvo, V. Pouthier, and C. Eilbeck, *Physica D* **221**, 58 (2006).
³¹J. P. Nguenang, R. A. Pinto, and S. Flach, *Phys. Rev. B* **75**, 214303 (2007).
³²P. Guyot-Sionnest, *Phys. Rev. Lett.* **67**, 2323 (1991).
³³R. Honke, P. Jakob, Y. J. Chabal, A. Dvorak, S. Tausendpfund, W. Stigler, P. Pavone, A. P. Mayer, and U. Schröder, *Phys. Rev. B* **59**, 10996 (1999).
³⁴R. P. Chin, X. Blase, Y. R. Shen, and S. GT. Louie, *Europhys. Lett.* **30**, 399 (1995).
³⁵P. Jakob, *Phys. Rev. Lett.* **77**, 4229 (1996).
³⁶P. Jakob, *Physica D* **119**, 109 (1998).
³⁷P. Jakob, *J. Chem. Phys.* **114**, 3692 (2001).
³⁸P. Jakob, *Appl. Phys. A: Mater. Sci. Process.* **75**, 45 (2002).
³⁹P. Jakob and B. N. J. Persson, *J. Chem. Phys.* **109**, 8641 (1998).
⁴⁰H. Okuyama, T. Ueda, T. Aruga, and M. Nishijima, *Phys. Rev. B* **63**, 233404 (2001).
⁴¹J. Edler, R. Pfister, V. Pouthier, C. Falvo, and P. Hamm, *Phys. Rev. Lett.* **93**, 106405 (2004).
⁴²J. Edler, V. Pouthier, C. Falvo, R. Pfister, and P. Hamm, in *Ultrafast Phenomena XIV*, edited by T. Kobayashi, T. Okada, T. Kobayashi, K. Nelson, and S. De Silvestri, *Springer Series in Chemical Physics*, Vol. 79 (Springer, Berlin, 2005).
⁴³S. Suntsov, K. G. Makris, D. N. Christodoulides, G. I. Stegeman, A. Hache, R. Morandotti, H. Yang, G. Salamo, and M. Sorel, *Phys. Rev. Lett.* **96**, 063901 (2006).
⁴⁴M. I. Molina, I. L. Garanovich, A. A. Sukhorukov, and Y. S. Kivshar, *Opt. Lett.* **31**, 2332 (2006).
⁴⁵E. Smirnov, M. Stepic, C. E. Rüter, D. Kip, and V. Shandarov, *Opt. Lett.* **31**, 2338 (2006).
⁴⁶K. G. Makris, S. Suntsov, D. N. Christodoulides, G. I. Stegeman, and A. Hache, *Opt. Lett.* **30**, 2466 (2005).
⁴⁷M. Stepic, E. Smirnov, C. E. Rüter, D. Kip, A. Maluckov, and L. Hadzievski, *Opt. Lett.* **32**, 823 (2007).
⁴⁸M. I. Molina, *Phys. Rev. B* **B71**, 035404 (2005).
⁴⁹S. K. Morrison and Y. S. Kivshar, *Opt. Commun.* **266**, 323 (2006).
⁵⁰C. Cohen-Tannoudji, J. Dupont-Roc, and G. Grynberg, *Atom-Photon Interactions: Basic Processes and Applications* (Wiley, New York, 1992).
⁵¹L. Dobrzynski, *Surf. Sci.* **299/300**, 1008 (1994).